Calculation of electron-potassium scattering

Igor Bray,* Dmitry V. Fursa, and Ian E. McCarthy
Electronic Structure of Materials Centre, School of Physical Sciences, The Flinders University of South Australia, G.P.O. Box 2100, Adelaide 5001, Australia
(Received 23 November 1992)

We present elastic through $7\,^2F$ differential, integrated, and total cross sections for electrons scattering from the ground state of potassium atoms. For the elastic channel, we also present spin asymmetries, and for the $4\,^2P$ channel we present spin asymmetries $L_\perp$ for singlet, triplet, and spin-averaged scattering, optical excitation cross sections, and various photon polarization observables. These are calculated using the coupled-channel optical method. A total of 17 target states are explicitly coupled with the effect of the continuum included in the first six of these. The calculations have been performed at a range of energies from 1 to 100 eV. The results are generally in good agreement with available experiment. We find that the effect of the inclusion of the continuum is most evident in calculating spin asymmetries and singlet $L_\perp$.

PACS number(s): 34.80.Bm, 34.80.Dp, 34.80.Nz

I. INTRODUCTION

Electron scattering by alkali metals provides an ideal testing ground for general theories of electron-atom scattering. From the theoretical point of view the more hydrogenlike an atom is the easier it is to treat with fewer approximations. From an experimental point of view the alkali-metal atoms are easier to produce than atomic hydrogen, though care must be taken due to their high chemical activity. As a result there is a great deal of both experimental and theoretical data on electron scattering by alkali metals. In this work we look at electron scattering on potassium with an emphasis on providing a systematic study across a broad energy range where the Born approximation is not applicable.

We use the coupled-channel optical (CCO) formalism of Bray, Konovalov, and McCarthy [1], which is a nonperturbative approach to electron-atom scattering. It is a generalization of the close-coupling (CC) method which explicitly couples only the first few discrete target states (P space) with the effect of the higher discrete and continuum states (Q space) being ignored. As such the CC method is generally applicable to low energies where only the considered channels are open. In the CCO method the effect of the remaining channels is not ignored but taken into account by the complex nonlocal polarization potential. This potential has a very complicated structure, but may be evaluated *ab initio* subject to the weak-coupling approximation. By this we mean that the potential is assumed to be diagonal in Q space. This results in the exclusion of only the effect on P space of interaction between distinct Q-space states. All other interactions are included. As a result the CCO method is applicable to all energies and has proved to be one of the most successful and general theories of electron-atom scattering to date. It has been thoroughly tested by comparison with experimental differential cross sections for hydrogen [1, 2], sodium [3, 4], and lithium [5]. It has also achieved remarkable agreement with the measurements of the spin-resolved $L_\perp$ parameters in sodium and spin asymmetries in sodium and lithium [5–7]. For the latter parameter the effect of the continuum was found to be very large in the intermediate energy region and yielded excellent agreement with experiment.

In this paper we apply our CCO formalism to electron scattering on potassium. This system has already received considerable attention (see the review of Bransden and McDowell [8], for example). The low energy region has been studied in detail by Moores [9] using the three-state $(4s, 4p, 3d)$ close-coupling model. His results superseded the two-state $(4s, 4p)$ close-coupling calculation of Karule and Peterkop [10]. These are in generally good agreement with experiment. In the intermediate energy region the Glauber-related approximations have been applied by Walters [11] to elastic and $4\,^2S$–$4\,^2P$ scattering, and by Gien [12] to elastic scattering. A distorted-wave approximation has been applied by Kennedy, Myerscough, and McDowell [13] to the $4\,^2S$–$4\,^2P$ transition. These calculations have been compared with their measurements of differential cross sections by Vušković and Srivastava [14] as well as the measurements by Buckman, Nobel, and Teubner [15]. The agreement between the various theories and experiment is not satisfactory. As the theories are based on high energy approximations it is likely that this is a major source for the discrepancies. A nonperturbative approach to the intermediate energy range was applied by Phelps *et al.* [16]. They performed a 15-state close-coupling calculation, in which exchange was neglected, and compared their results for the integrated cross sections with their measurements. These were found to be better for the lower-lying channels, and improved with higher energies.

In this paper we present 17-state close-coupling calculations that treat exchange fully as well as take into account the effect of the continuum. We also study the effect of small variation in the structure approximation of the potassium atom on our results.

In Sec. II we give a qualitative description of the CCO

method, since it has been derived elsewhere. In Sec. III we present the results of our CCO calculations which have been performed at a range of projectile energies of 1–100 eV incident on the ground state of potassium, and compare them with available measurements of the following:

(i) Differential cross sections of the elastic $4\,^2S$, and the inelastic $4\,^2P$, $5\,^2S+3\,^2D$, $5\,^2P$, $4\,^2D+6\,^2S+4\,^2F+6\,^2P$, and $5\,^2D+7\,^2S+5\,^2F$ channels at 7, 20, 40, 60, and 100 eV.

(ii) The optical excitation cross section and the polarization function of the $4\,^2P$ channel from threshold to 100 eV.

(iii) The ratios of photon circular polarization to electron spin polarization for total angular momentum $j = 1/2$ and $j = 3/2$, as well as direct excitation cross sections for magnetic sublevels $m_L = 0$ and $m_L = 1$ for the $4\,^2P$ channel at energies ranging from threshold to 20 eV.

Though we are unaware of any measurements of spin asymmetries we present our results for the elastic and $4\,^2P$ channels at 7, 10, and 20 eV. At these energies we also present calculations of the angular momentum transferred to the atom perpendicular to the scattering plane for singlet $L_\perp^S$, triplet $L_\perp^T$, and spin-averaged $L_\perp$ scattering.

II. THEORY

We make the approximation that the problem of electron scattering by potassium may be treated as a three-body problem. The three bodies are taken to be the frozen core together with the valence and projectile electrons. The formal derivation of the CCO equations for such systems has been given by Bray, Fursa, and McCarthy [5]. A finite set of discrete target states is treated directly via the close-coupling formalism, with the effect of the continuum being included via a complex nonlocal polarization potential. The partial-wave matrix elements of this polarization potential are given by Bray, Konovalov, and McCarthy [1]. The two electrons are assumed to move in the frozen-core Hartree-Fock (FCHF) potential to which we add a small phenomenological core-polarization potential which represents virtual excitations of the core. This two-parameter local potential is used to considerably improve the one-electron energies.

We use the form of the polarization potential $v_{\rm pol}$ given by Zhou *et al.* [17]

$$v_{\rm pol}(r) = \frac{-\alpha}{2r^4}\{1 - \exp[-(r/\rho)^6]\}, \qquad (1)$$

where α and ρ are determined by fitting to the lowest-lying experimental one-electron energies. Note that the same values of α and ρ apply for all partial waves of $|\phi_j\rangle$. For potassium we take $\alpha = 5.354a_0^3$ (the static dipole polarizability [18]), and $\rho = 2.0a_0$. To check the dependence of our results for scattering observables on the form of this potential we also performed the calculations with $\alpha = 6.5a_0^3$ and $\rho = 2.5a_0$. This set also gives good one-electron energies and was chosen as it yields a better energy for the $3d$ target state (see discussion in Sec. III). The resulting one-electron energies for the two sets of α and ρ in (1), as well as the frozen-core Hartree-Fock ($\alpha = 0$) model, are given in Table I.

The coupled CCO equations are written in momentum space as a set of coupled Lippmann-Schwinger equations. These are integral equations which we solve using the partial-wave expansion in the total orbital angular momentum, and using the distorted-wave representation for the projectile electron. The distorted-wave representation is a purely numerical technique which reduces the number of momentum quadrature points in the solution of the integral equations; see Bray *et al.* [19] for more detail. We utilize around 40 quadrature points in each channel in solving the coupled integral equations.

The LS coupling scheme is used, and so the singlet ($S = 0$) and triplet ($S = 1$) channels form a separate set of coupled equations. For potassium we take P space to contain the 17 states of Table I. In this table we give three sets of energies corresponding to the calculation of the states above the frozen core with ($\rm FCHF_1^+$, $\rm FCHF_2^+$), and without (FCHF) the phenomenological polarization potential (1). We see that the FCHF model yields good one-electron energies only for the high-lying target states, with the $\rm FCHF^+$ models providing considerable improvement for the low-lying states. We found that our results for the two sets of $\rm FCHF^+$ are very similar, but these are often significantly different from those with the FCHF wave functions. In all work presented here the $\rm FCHF_1^+$ wave functions are used. The one-electron energies of these are quite good, but pose a limitation on a detailed

TABLE I. Ionization energies (eV) of the potassium target states used in the 17CC and 17CCO6 calculations. The wave functions are calculated in the frozen-core Hartree-Fock model with an added phenomenological polarization potential given in Eq. (1). The wave functions denoted by $\rm FCHF_1^+$ and $\rm FCHF_2^+$ have $\alpha = 5.354a_0^3$, $\rho = 2.0a_0$ and $\alpha = 6.5a_0^3$, $\rho = 2.5a_0$, respectively. For contrast we also present the pure frozen-core Hartree-Fock results ($\alpha = 0.0$) which are denoted by FCHF. The experimental values are due to Moore [30].

	Energy (eV)			
State	FCHF	$\rm FCHF_1^+$	$\rm FCHF_2^+$	Expt.
$4s$	4.013	4.348	4.336	4.339
$5s$	1.661	1.734	1.728	1.733
$6s$	0.910	0.937	0.934	0.937
$7s$	0.574	0.587	0.586	0.587
$4p$	2.604	2.728	2.734	2.729
$5p$	1.241	1.276	1.277	1.277
$6p$	0.729	0.744	0.744	0.744
$7p$	0.480	0.488	0.488	0.488
$3d$	1.585	1.725	1.687	1.671
$4d$	0.896	0.977	0.949	0.943
$5d$	0.572	0.616	0.600	0.598
$6d$	0.395	0.421	0.412	0.411
$7d$	0.289	0.305	0.299	0.299
$4f$	0.850	0.853	0.854	0.853
$5f$	0.544	0.546	0.546	0.545
$6f$	0.378	0.379	0.379	0.379
$7f$	0.278	0.278	0.278	0.278

study of scattering phenomena, particularly near thresholds.

The 17 states used in our calculations are sufficient to demonstrate convergence in the expansion of the total wave function using just the discrete target states. By this we mean that for all of the observables under consideration in this work further increase in the number of discrete target states does not yield significantly different results. With this many discrete states we take Q space to be only the target continuum.

As the coupled Lippmann-Schwinger equations are expanded in partial waves of total orbital angular momentum it is necessary to ensure that sufficient partial waves are considered. The number of partial waves taken varies with the projectile energy. For energies ranging from 1 to 100 eV we solve the coupled integral equations explicitly from 10 to 100 partial waves, respectively. We also utilize the fact that for high partial waves the inelastic T-matrix elements converge to the Born matrix elements, and so we perform an analytic Born subtraction as described by McCarthy and Stelbovics [20]. This results in the complete set of partial waves being used, which is particularly important for the $4\,^2P$ channel.

The effect of Q space on the scattering is taken into account by the complex nonlocal polarization potential V_Q^S. In calculating its matrix elements [1] we utilize 15 continuum target states to integrate over the continuum energy, for each target partial wave up to $l = 5$. These elements are calculated for each partial wave of total orbital angular momentum, and take up to 95% of the calculation time. The computational time varies with the number of P-space channels that have coupling to the continuum via V_Q^S. Given the large number of P-space states taken we are unable, for computational considerations, to include the coupling to the continuum in all of these states. In our previous work on lithium [5] and sodium [7] we found that coupling of the first six target states to the continuum was sufficient for convergence in observable phenomena for the low-lying target states. This is the case for potassium also. The effect on the high-lying target states presented here is difficult to estimate and will be discussed at a later stage. We denote our calculations by 17CCO6 and 17CC, with the latter being used to simply show what effect if any the inclusion of coupling to the continuum has on the scattering of interest.

III. RESULTS

We have performed our calculations at a range of energies from 1 to 100 eV. The low energy region (< 5 eV) has been adequately addressed by the three-state calculations of Moores [9]. As these calculations are valid at these energies our results show no significant improvement there, but are in good agreement with the much earlier calculations. Rather than presenting the low energy results in detailed pictorial form we concentrate on presenting the results in the intermediate and high energy regions where there are little reliable theoretical results available.

A. Integrated cross sections

In Fig. 1 we present the optical excitation cross section of the $4\,^2P$ channel from threshold of 1.6 eV to 100 eV. This cross section is measured by observing photons emitted by the deexcitation of the $4\,^2P$ state. This cross section is the sum of the $4\,^2P$ cross section together with the cross sections of the higher excited states which have cascaded to the $4\,^2P$ state. As the $3\,^2D$ and $5\,^2S$ states primarily deexcite via the $4\,^2P$ state, the optical excitation cross section for the $4\,^2P$ channel of potassium is given mostly by the sum of just the $4\,^2P$, $3\,^2D$, and $5\,^2S$ cross sections.

Our 17CCO6 ($4\,^2P + 3\,^2D + 5\,^2S$) calculation is in excellent agreement with measurements of Chen and Gallagher [21] and Phelps *et al.* [16] at all energies except in the vicinity of 2 eV. Comparing this calculation with the corresponding 17CC result shows that the inclusion of continuum target states has the largest effect in the energy region of 10–40 eV, and improves agreement with experiment. Comparing with the 17CCO6 result for just the $4\,^2P$ channel we see that, at energies above the $3\,^2D$ and $5\,^2S$ thresholds (2.6 eV), cascades to the $4\,^2P$ channel may be as high as 20%. The 17CCO6 ($4\,^2P+3\,^2D+5\,^2S$, FCHF) calculation utilizes the FCHF wave functions and shows the very large effect that the polarization potential

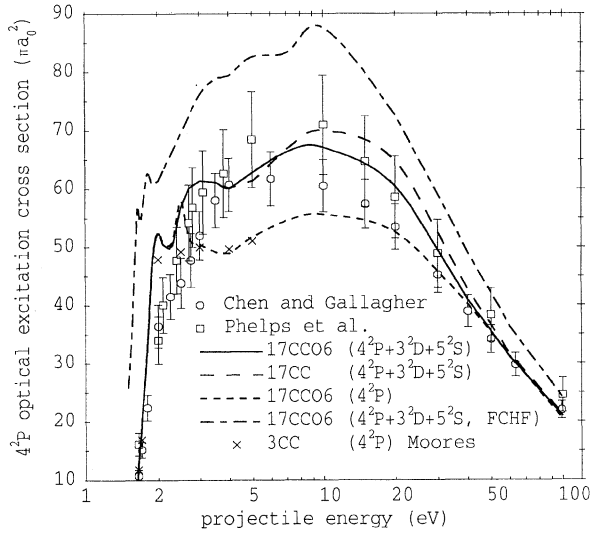

FIG. 1. The $4\,^2P$ optical excitation cross section, i.e., the $4\,^2P$ cross section plus cascades. The measurements denoted by ○ and □ are due to Chen and Gallagher [21] and Phelps *et al.* [16], respectively. The 17CCO6 and 17CC calculations use the 17 states given in Table I, with the 17CCO6 calculation also including the effect of continuum on the six lowest-lying states. The three-state ($4s, 4p, 3d$) calculation of Moores [9] is denoted by ×. All of the calculations, except for the one denoted by FCHF, utilize the FCHF_1^+ wave functions. See Table I for more detail. The difference between the $4\,^2P$ and $4\,^2P + 3\,^2D + 5\,^2S$ calculations indicates the cascade contribution to the $4\,^2P$ cross section. Quantitative results may be obtained by correspondence with the first author.

(1) has on the results.

Our results are in good agreement with Moores [9] at just above the 4^2P threshold and above the cascades threshold. In the energy region between the 4^2P and the cascades threshold there is discrepancy between experiment and theory. Our calculations and those of Moores are above experiment in this region. To test the stability of our results we have performed the calculation in this energy region using both sets of the $FCHF^+$ wave functions given in Table I. Even though the two sets have slightly different energies for the $3d$ target state, they yield very similar results. So the demonstrated theoretical structure is quite stable. We suggest the following possible cause for the discrepancy. Both sets of measurements have a finite energy resolution, 0.25 eV for Chen and Gallagher [21] and 0.75 eV for Phelps *et al.* [16]. At just above 1.6 eV the cross section increases linearly and so the finite energy resolution does not cause any problems. As the energy is increased the cross section levels out quite rapidly, with a finite energy resolution leading to an underestimation of the cross section.

To find the origin of the discrepancy with the result of Moores at 2.5 eV, we first performed the same three-state $(4s, 4p, 3d)$ calculation and obtained his result to within 3%. This indicates that there is not a great difference in the choice of target wave function used by him and us. This is also confirmed by the fact that we get similar results at even lower energies as well. We then proceeded to add the $5s$ state and found that the resulting four-state calculation was very similar to the presented 17-state ones. This explains the discrepancy between our result and that of Moores at this energy.

The quantitative results of the integrated cross sections at selected energies where there exist considerable experimental data are presented in Table II. They are compared with the estimates of Vušković and Srivastava

TABLE II. Integrated cross sections (in units of a_0^2) for electron scattering on the ground state of potassium. The theoretical results are denoted by 17CCO6. The measurements denoted by Expt1, Expt2, Expt3 are due to Vušković and Srivastava [14], Phelps *et al.* [16], and Kwan *et al.* [22], respectively.

		Energy (eV)					
Channel	Method	5	7	20	40	60	100
4^2S	17CCO6	230	151	69.9	48.3	38.9	28.9
	Expt1		170±34	62.9±13	55.4±11	37.9±7.6	15.8±3.2
4^2P	17CCO6	157	168	164	114	87.5	59.7
	Expt1		179±36	164±33	113±23	87.5±18	62.1±12
	Expt2	143±21	157±24	148±22	111±17	93.5±14	66.1±10
3^2D	17CCO6	33.3	34.1	22.3	11.9	8.00	4.84
	Expt2	30.3±6	30.7±6.1	19.4±3.9	11.5±2.3	8.13±1.6	5.5±1.1
5^2S	17CCO6	6.60	6.65	3.33	2.34	1.82	1.21
	Expt2	11.5±5.8	8.82±4.4	3.25±1.6	2.54±1.3	1.78±0.9	1.51±0.8
$5^2S + 3^2D$	17CCO6	39.9	40.8	25.6	14.2	9.82	6.05
	Expt1		49.9±10	24.3±4.9	16.0±3.2	10.6±2.1	4.79±1.0
	Expt2	41.8±6	39.5±6.1	22.7±3.9	14.0±2.3	9.91±1.6	7.01±1.1
5^2P	17CCO6	7.29	6.75	4.04	2.93	2.22	1.49
	Expt1		5.18±1.0	4.07±0.8	2.29±0.5	1.68±0.3	0.79±0.2
	Expt2	9.1±2.7	8.18±2.5	5.50±1.7	3.29±1.0	2.64±0.8	1.76±0.5
4^2D	17CCO6	7.07	5.97	2.05	1.14	0.79	0.50
4^2F	17CCO6	4.55	5.62	1.55	0.61	0.36	0.19
6^2S	17CCO6	2.88	3.32	1.05	0.62	0.44	0.25
	Expt2	1.69±0.7	1.31±0.5	0.64±0.3	0.49±0.2	0.39±0.2	0.26±0.1
6^2P	17CCO6	2.72	2.77	1.44	0.83	0.58	0.37
	Expt2	1.72±0.7	1.43±0.6	0.95±0.4	0.57±0.2	0.40±0.2	0.32±0.1
$4^2D + 4^2F + 6^2S + 6^2P$	17CCO6	17.2	17.7	6.09	3.20	2.17	1.31
	Expt1		12.0±4.8	5.18±2.1	2.11±0.8	1.39±0.6	0.50±0.2
5^2D	17CCO6	2.03	3.06	0.70	0.35	0.23	0.13
	Expt2	2.39±1.0	2.02±0.8	0.91±0.4	0.51±0.2	0.37±0.1	0.24±0.1
5^2F	17CCO6	2.86	3.29	0.83	0.32	0.19	0.11
	Expt2	1.85±0.6	1.57±0.5	0.64±0.2	0.34±0.1	0.24±0.07	0.14±0.04
7^2S	17CCO6	1.10	1.60	0.48	0.27	0.18	0.11
	Expt2	0.79±0.2	0.64±0.2	0.29±0.1	0.21±0.1	0.17±0.05	0.11±0.03
$5^2D + 5^2F + 7^2S$	17CCO6	5.99	7.95	2.01	0.94	0.60	0.35
	Expt1		4.21±1.7	2.07±0.8	1.04±0.4	0.53±0.2	0.25±0.1
	Expt2	5.03±1.0	4.23±0.8	1.84±0.4	0.95±0.2	0.78±0.1	0.49±0.1
σ_t	17CCO6	469	409	289	198	151	103
	Expt1		439±88	293±59	214±43	157±31	100±20
	Expt3	321±64	314±66	238±50	158±33	145±30	114±24

[14], Phelps *et al.* [16], and Kwan *et al.* [22]. A more comprehensive set in the energy range from 1 to 100 eV may be obtained by correspondence with the first author.

We generally find excellent agreement between our results and the measurements. Where two sets of measurements are in disagreement one of these tends to be favored by our results. On some occasions there is substantial disagreement between theory and experiment. We will address these cases in more detail when discussing the differential cross sections.

B. Polarization and direct excitation

Apart from measuring optical excitation cross sections of the $4\,^2P$ channel, Chen and Gallagher [21] and Phelps *et al.* [16] also measured the polarization of the emitted photons. Ludwig *et al.* [23] used these results together with their measurements of the ratio of the circular polarization P_j^σ of light emitted in the forward direction to electrons spin polarized longitudinally with degree P_e, to yield the magnetic sublevel-dependent direct excitation cross section D_{m_L} (see Moores and Norcross [24] for definition).

In Fig. 2 we present the polarization function P' of the $4\,^2P$ channel from threshold to 100 eV. For potassium P' has been evaluated by Ludwig *et al.* [23] to be given by

$$P' = \frac{Q_0 - Q_1}{4.02Q_0 + 7.04Q_1}, \tag{2}$$

where Q_0 and Q_1 are the magnetic sublevel integrated cross sections. Comparison of the 17CCO6 and 17CC theories indicates that the effect of continuum is very small. Our results are in better agreement with the measurements of Chen and Gallagher [21] than Phelps *et al.* [16].

The measured ratios P_j^σ/P_e for total angular momentum $j = 1/2$ and $j = 3/2$, Ludwig *et al.* [23] expressed as

$$P_{3/2}^\sigma/P_e = \frac{Q_0 - D_0 + 4(Q_1 - D_1)}{2.66Q_0 + 7.08Q_1} \tag{3}$$

in the transition $4\,^2P_{3/2} \rightarrow 4\,^2S_{1/2}$, and

$$P_{1/2}^\sigma/P_e = 0.4\frac{Q_0 - D_0 - 2(Q_1 - D_1)}{Q_0 + 2Q_1} \tag{4}$$

in the transition $4\,^2P_{1/2} \rightarrow 4\,^2S_{1/2}$, where D_{m_L}, $m_L = 0, 1$ are the direct excitation cross sections. In deriving (2), (3), and (4) Ludwig *et al.* [23] take account of fine and hyperfine structure according to the work of Percival and Seaton [25] and Flower and Seaton [26]. Using the relation for the total (integrated) $4\,^2P$ cross section

$$Q = Q_0 + 2Q_1, \tag{5}$$

they also expressed the direct excitation cross sections in terms of only measured quantities as

$$D_0 = \frac{Q}{3 - P'}[\,1 + 7.04P' - 1.66(3 - P')P_{1/2}^\sigma/P_e - 3.25(1 - P')P_{3/2}^\sigma/P_e] \tag{6}$$

and

$$D_1 = \frac{Q}{3 - P'}[\,1 - 4.02P' + 0.41(3 - P')P_{1/2}^\sigma/P_e - 1.62(1 - P')P_{3/2}^\sigma/P_e]. \tag{7}$$

In Fig. 3 we compare our results for the $P_{3/2}^\sigma/P_e$ and $P_{1/2}^\sigma/P_e$ ratios, as well as D_0 and D_1 with experiment and results of Moores. In presenting D_0 and D_1 Lud-

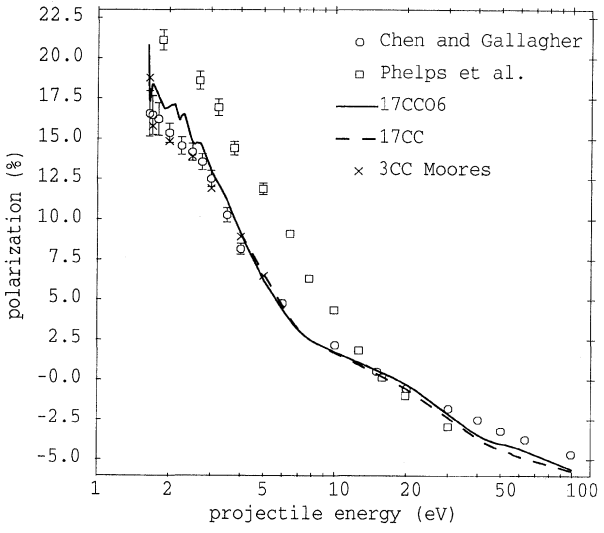

FIG. 2. The polarization percentage of the radiation of the $4p$ state of potassium on electron impact. Theory and experiment are as for Fig. 1. Error bars are only plotted if larger than the size of symbol denoting the experiment.

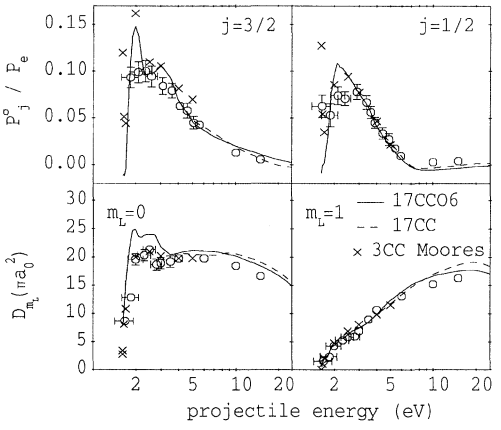

FIG. 3. Circular polarization P_j^σ/P_e of the $4\,^2P_j \rightarrow 4\,^2S_{1/2}$ component of potassium-resonance radiation for $j = 1/2, 3/2$, and direct excitation cross sections D_{m_L} for $m_L = 0, 1$. The theory is as for Fig. 1. The measurements are due to Ludwig *et al.* [23]. We have corrected their measurements of D_{m_L} for cascade contributions (see Fig. 1). Error bars are only plotted if larger than the size of the symbol denoting the experiment.

wig *et al.* [24] used the Q and P' values of Chen and Gallagher. They had assumed that the cascade contribution to the total cross section for $4\,^2P$ excitation Q would be very small. As we have shown that this is not the case we have renormalized their results accordingly. This leads to much better agreement between the theories and experiment for the larger energies (cf. Figs. 7 and 8 of [24]).

The major discrepancy of our results with those of experiment is in the region of 2 eV. We checked our results by using both sets of $FCHF^+$ wave functions, and found the same qualitative behavior. As with the integrated $4\,^2P$ cross section, we were able to reproduce the results of Moores using the same three-state calculation, but on adding the $5s$ state the results altered significantly to be similar to the 17-state results presented. Given that the energy resolution in the experiment is quite broad, it is difficult to determine the cause of the discrepancy of our calculations with experiment in this energy region.

C. Differential cross sections

In this section we present the differential cross sections for the elastic, $4\,^2P$, $5\,^2S+3\,^2D$, $5\,^2P$, $4\,^2D+6\,^2S+4\,^2F+6\,^2P$, and $5\,^2D+7\,^2S+5\,^2F$ channels at a range of projectile energies incident upon potassium in the ground state, and compare with available measurements. In Fig. 4 we present the differential cross sections at 7 eV. For the elastic channel we see remarkable agreement of both the 17CCO6 and 17CC results with the relative measurements of Gehenn and Wilmers [27]. Agreement with the measurements of Vušković and Srivastava [14] is quite poor at the intermediate angles not only for the elastic, but all of the presented inelastic channels. To test the stability of the results we performed the calculations with all three sets of wave functions of Table I, and also performed a 21-state calculation that had an extra s, p, d, and f state. The variation between these was considerably smaller than between experiment and the presented 17-state results. Though the elastic measurements of Gehenn and Wilmers [27] were much earlier than those of Vušković and Srivastava [14], excellent agreement with their results we find encouraging.

The very small difference between the 17CCO6 and 17CC results indicates that continuum states have little effect on the differential cross sections at this energy. It may be argued that the effect of the continuum may be more important for the higher-lying states. All of the states in the four leftmost pictures had coupling to the continuum included. The large discrepancy between theory and experiment for say the $5\,^2P$ channel suggests to us that a lack of continuum couplings is not the source of the discrepancies. The poor agreement with the higher-channel differential cross sections also leads to not very good agreement with the integrated cross sections given in Table II.

The differential cross sections at 20 eV are given in Fig. 5. The agreement with measurements of Vušković and Srivastava [14] is quite good for all channels, a considerable improvement on the situation at 7 eV. As our theory is applicable at all energies we do not consider the 20-eV results any more reliable than the 7-eV ones. Comparison of the 17CCO6 and 17CC calculations indicates that the continuum does not have a great influence at this energy either, but tends to improve agreement with experiment. Associated integrated cross sections given in Table II are also in excellent agreement with experiment.

In Fig. 6 we look at the differential cross sections of 40-eV electrons scattering on the ground state of potassium. We see good agreement with experiment of the two theories for all channels at the forward and intermediate angles. Theory consistently predicts larger cross sections than experiment at backward angles. Looking at Table

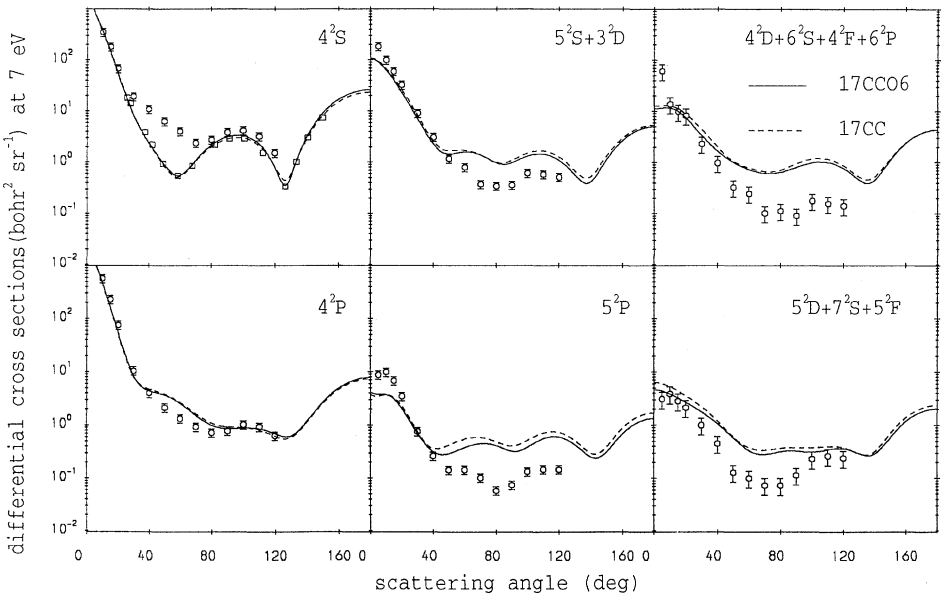

FIG. 4. Differential cross sections for electron scattering on potassium at 7 eV projectile energy. Theory is as for Fig. 1. The relative measurements of Gehenn and Wilmers [27] are denoted by □. The measurements of Vušković and Srivastava [14] are denoted by ○.

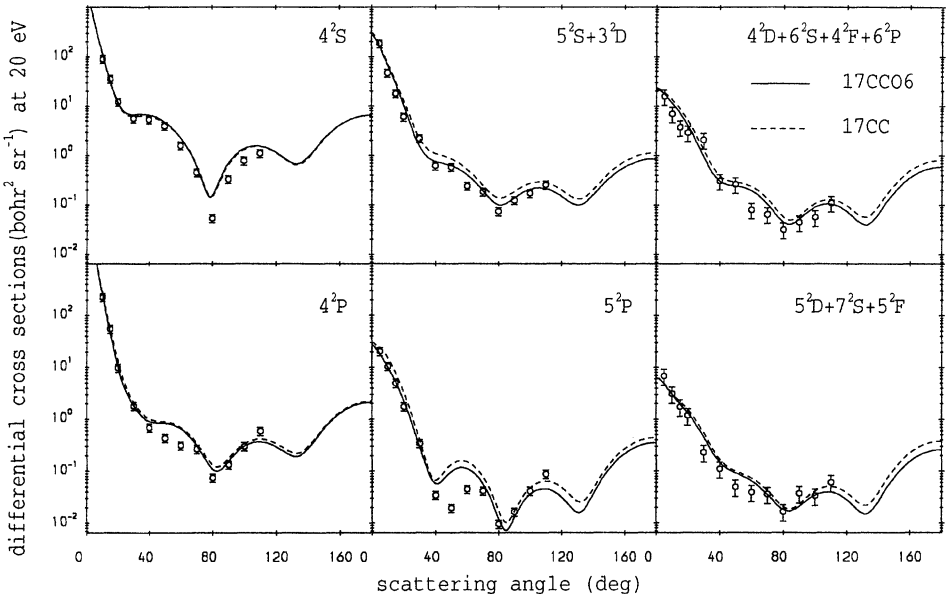

FIG. 5. Differential cross sections for electron scattering on potassium at 20 eV projectile energy. Theory and experiment are as for Fig. 4.

II we see that these discrepancies do not affect the integrated cross sections as agreement with experiment is quite good.

In Figures 7 and 8 we present the differential cross sections for projectile energies of 60 and 100 eV, respectively. Comparison of the 17CCO6 and 17CC results indicates that the already small effect of the continuum on the differential cross sections diminishes with increasing energy. In addition to the measurements of Vušković and Srivastava [14] there are measurements of the elastic and $4\,^2P$ differential cross sections at 54.4 and 100 eV by Buckman, Nobel, and Teubner [15]. We have compared our 54.4- and 60-eV calculations and found little visible difference. We assume this to be the case experimentally also, and so present their 54.4-eV data for comparison. At 60 eV there are also the measurements of Williams and Trajmar [28] for the elastic, $4\,^2P$, and $5\,^2S + 3\,^2D$ channels. We see that there is some discrepancy between theory and experiment. There are some significant discrepancies between the different experiments also. At these high energies the theory is rapidly convergent in the number of target states used, as well as being insensitive to the choice of the $FCHF^+$ wave functions. It is therefore a surprise to us to find poor agreement with experiment at the intermediate and backward angles. As the integrated cross sections are dominated by the for-

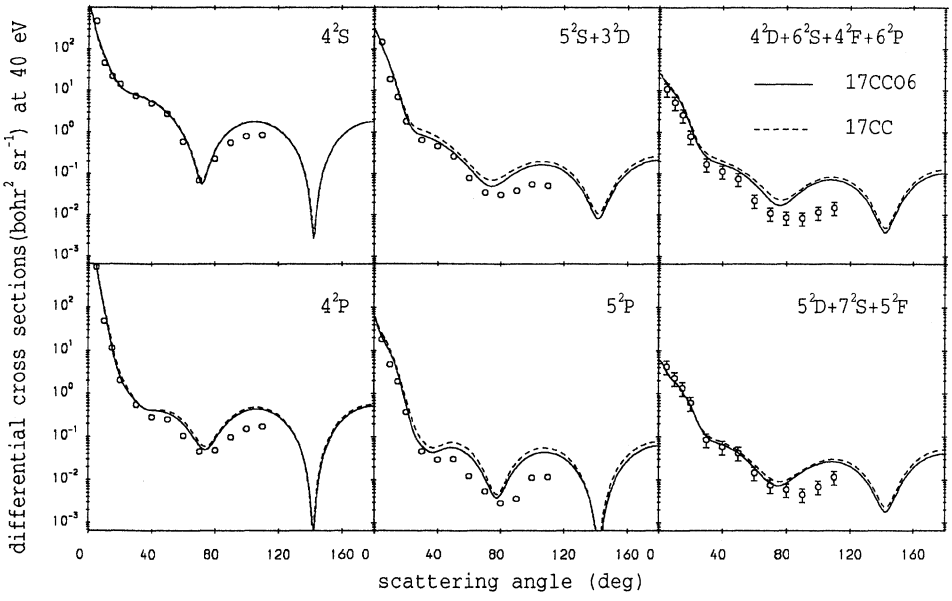

FIG. 6. Differential cross sections for electron scattering on potassium at 40 eV projectile energy. Theory and experiment are as for Fig. 4.

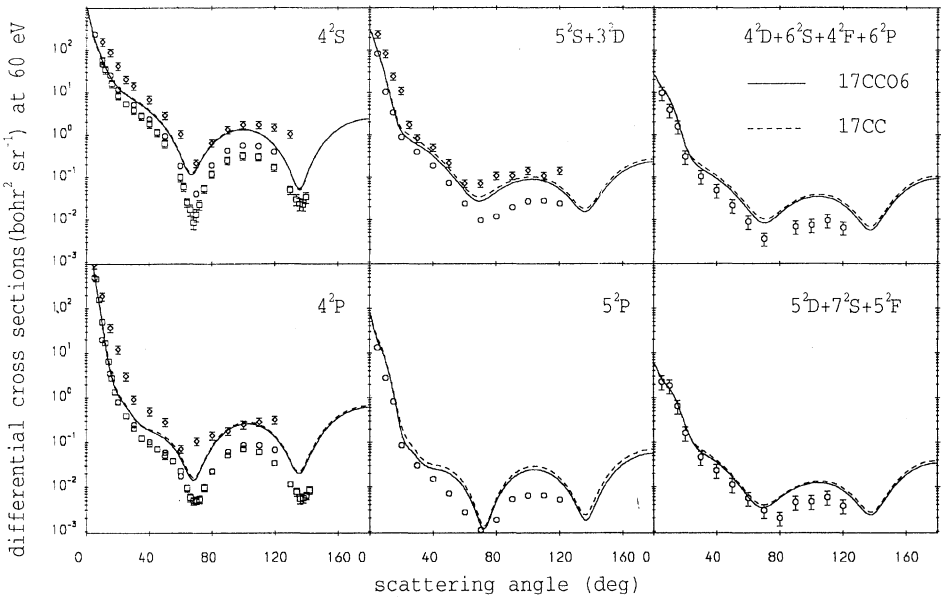

FIG. 7. Differential cross sections for electron scattering on potassium at 60 eV projectile energy. The theory is as for Fig. 4. The measurements of Vušković and Srivastava [14], Buckman, Nobel, and Teubner [15] (at 54.4 eV), and those of Williams and Trajmar [28] are denoted by ○, □, and ◇, respectively.

ward angles, we find generally good agreement between experimental and theoretical integrated cross sections in Table II.

The situation is similar to that found in electron scattering on sodium; see Bray, Konovalov, and McCarthy [4] for example. There at the same energies the theory is considerably higher than some of the experiments at the intermediate and backward angles. However, there are also measurements which are in good agreement with theory. The measurements of Williams and Trajmar are in better agreement with our results at these angles, but this is of little comfort given the poor agreement at forward angles. As with sodium, the variation between different experiments suggests the difficulty of making accurate measurements of differential cross sections across an angular range where count rates drop many orders of magnitude.

D. Spin asymmetries and $L_\perp$

Writing the singlet and triplet scattering cross sections as $|S|^2$ and $|T|^2$, respectively, spin asymmetry A_{ex} is related to the ratio of triplet to singlet scattering $r = |T|^2/|S|^2$ by

$$A_{ex} = \frac{1-r}{1+3r}. \tag{8}$$

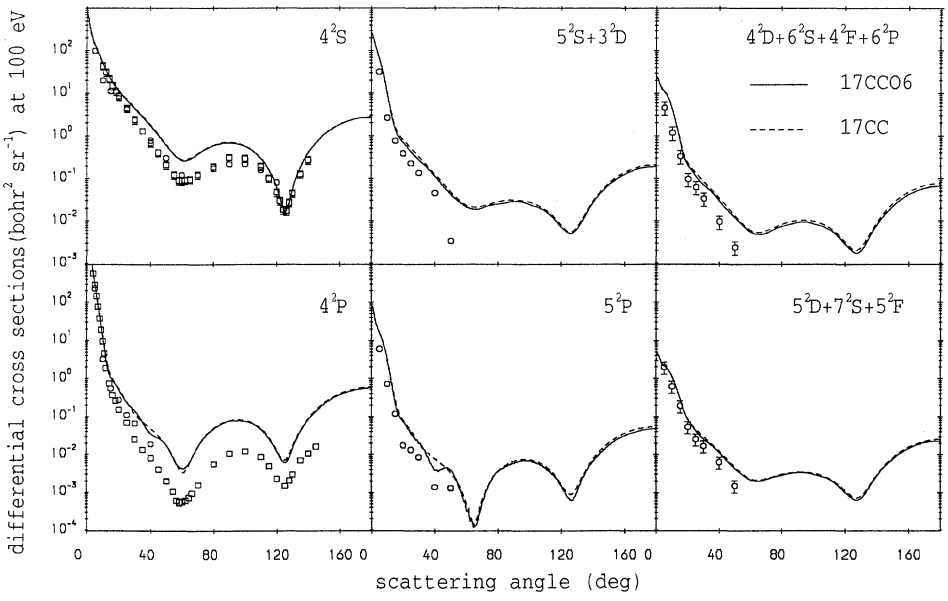

FIG. 8. Differential cross sections for electron scattering on potassium at 100 eV projectile energy. Theory and experiment are as for Fig. 7.

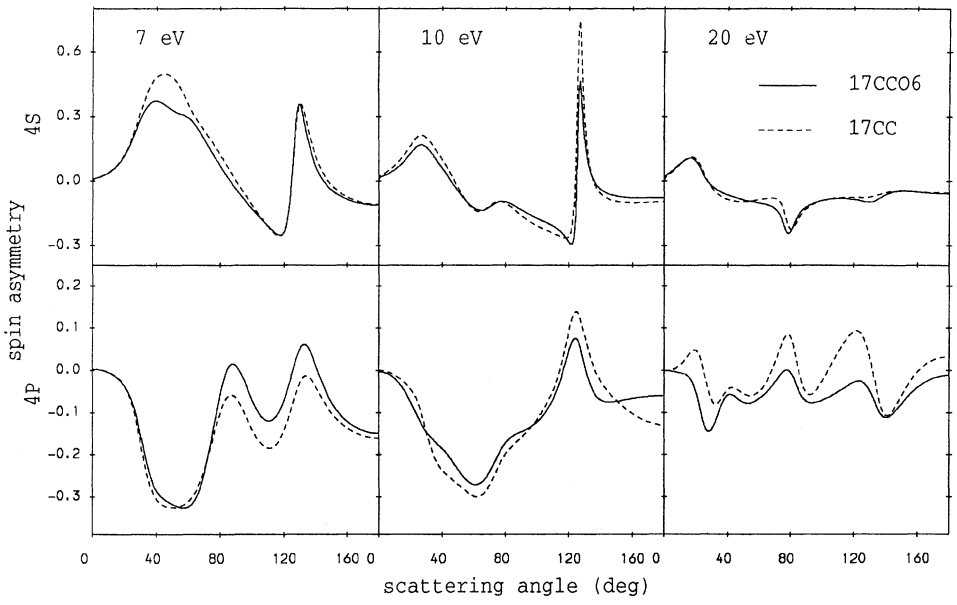

FIG. 9. Differential elastic and 4^2P spin asymmetries for electron scattering on potassium at 7, 10, and 20 eV projectile energies. The theory is as for Fig. 1. The difference between the two calculations indicates the effect of the inclusion of continuum in the close-coupling expansion.

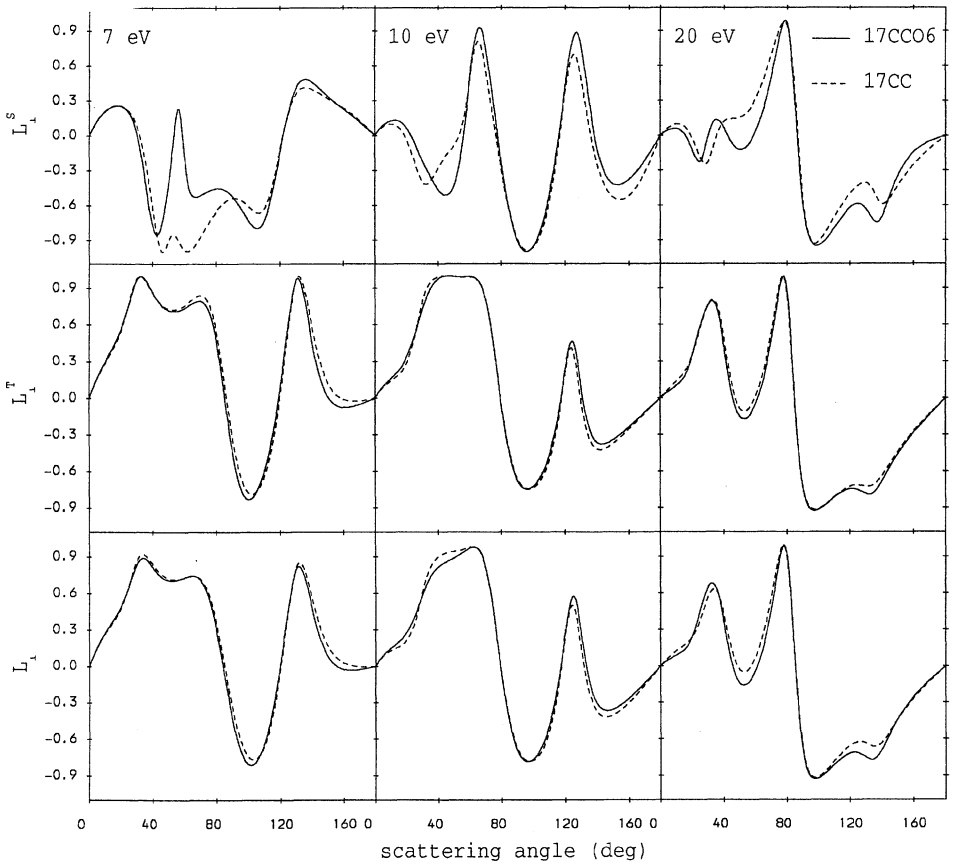

FIG. 10. Angular momentum transferred to the atom perpendicular to the scattering plane for singlet $L_\perp^S$, triplet $L_\perp^T$, and spin-averaged $L_\perp$ scattering at incident projectile energies of 7, 10, and 20 eV for the 4^2P state of potassium. The theory is as for Fig. 9.

For the $4\,^2P$ channel, in the natural coordinate frame [29], the singlet and triplet amplitudes may be written as S_{m_L} and T_{m_L} for $m_L = 1, -1$. The angular momentum transferred to the atom perpendicular to the scattering plane is then given by

$$L_\perp^S = \frac{|S_{+1}|^2 - |S_{-1}|^2}{|S_{+1}|^2 + |S_{-1}|^2} \tag{9}$$

for singlet scattering,

$$L_\perp^T = \frac{|T_{+1}|^2 - |T_{-1}|^2}{|T_{+1}|^2 + |T_{-1}|^2} \tag{10}$$

for triplet scattering, and

$$L_\perp = \frac{|S_{+1}|^2 - |S_{-1}|^2 + 3(|T_{+1}|^2 - |T_{-1}|^2)}{|S_{+1}|^2 + |S_{-1}|^2 + 3(|T_{+1}|^2 + |T_{-1}|^2)} \tag{11}$$

for spin-averaged scattering.

In Figs. 9 and 10 we present 17CCO6 and 17CC calculations of the A_{ex} and $L_\perp$ parameters at 7, 10, and 20 eV. We are not aware of any measurements of these parameters for potassium at this time. Having found excellent quantitative agreement between our theory and the measurements of these parameters in sodium [7], we present them here for completeness, and to see if the effect of the continuum is as large as it is for sodium.

We see that the effect of the continuum on these parameters is quite noticeable, for instance in the 7-eV $L_\perp^S$ parameter. As these parameters result from measurements of ratios at each angle they do not suffer from the same difficulties as do differential cross sections, and may be experimentally determined to an accuracy of order of a few percent. Thus, the visible difference between the 17CCO6 and 17CC calculations should be readily discriminated by experiment in favor of the former.

IV. CONCLUSIONS

We have applied our CCO theory to electron scattering on potassium. We found generally good agreement with experiment across the energy range considered of 1–100 eV. In the case where agreement is not good there is reason to believe that the problems may be due to difficulties in the experiment. We believe this because we have tested the stability of our results upon variation of wave functions, and have used as many target states as necessary for convergence in the expansion using discrete states. We have also incorporated the effect of the continuum. We therefore have included all of the physics necessary to describe electron-atom scattering. We are also encouraged in this belief by the excellent agreement of similar calculations with spin-dependent experiments on sodium [7].

It is our intention to expand our codes to handle two-electron atoms as well as to be able to provide results for scattering from excited p target states. These projects are currently being implemented.

ACKNOWLEDGMENTS

We acknowledge support from the Australian Research Council. One of us (D.V.F.) acknowledges financial support from The Flinders University of South Australia.

* Electronic mail: igor@esm.cc.flinders.edu.au

[1] I. Bray, D. A. Konovalov, and I. E. McCarthy, Phys. Rev. A **43**, 5878 (1991).
[2] I. Bray, D. A. Konovalov, and I. E. McCarthy, Phys. Rev. A **44**, 5586 (1991).
[3] I. Bray, D. A. Konovalov, and I. E. McCarthy, Phys. Rev. A **44**, 7830 (1991).
[4] I. Bray, D. A. Konovalov, and I. E. McCarthy, Phys. Rev. A **44**, 7179 (1991).
[5] I. Bray, D. V. Fursa, and I. E. McCarthy, Phys. Rev. A **47**, 1101 (1993).
[6] I. Bray, Phys. Rev. Lett. **69**, 1908 (1992).
[7] I. Bray and I. E. McCarthy, Phys. Rev. A **47**, 317 (1993).
[8] B. H. Brandsen and M. R. McDowell, Phys. Rep. **46**, 249 (1978).
[9] D. L. Moores, J. Phys. B **9**, 1329 (1976).
[10] E. M. Karule and R. K. Peterkop, in *Atomic Collisions III*, edited by Y. Ia. Veldre (Latvian Academy of Sciences, Riga, USSR, 1965)[JILA Information Center Report No. 3, University of Colorado, Boulder, CO], pp. 1–27; E. M. Karule, *ibid.* pp. 29–48.
[11] H. R. J. Walters, J. Phys. B **6**, 1003 (1973).
[12] T. T. Gien, J. Phys. B **21**, 3767 (1988).
[13] J. V. Kennedy, V. P. Myerscough, and M. R. C. McDowell, J. Phys. B **10**, 3759 (1977).
[14] L. Vušković and S. K. Srivastava, J. Phys. B **13**, 4849 (1980).
[15] S. J. Buckman, C. J. Nobel, and P. J. O. Teubner, J. Phys. B **12**, 3077 (1979).
[16] J. O. Phelps, J. E. Solomon, D. F. Korff, and C. C. Lin, Phys. Rev. A **20**, 1418 (1979).
[17] H. L. Zhou, B. L. Whitten, G. Snitchler, and D. W. Norcross, Phys. Rev. A **42**, 3907 (1990).
[18] W. Müller, J. Flesch, and W. Meyer, J. Chem. Phys. **80**, 3297 (1984).
[19] I. Bray, I. E. McCarthy, J. Mitroy, and K. Ratnavelu, Phys. Rev. A **39**, 4998 (1989).
[20] I. E. McCarthy and A. T. Stelbovics, Phys. Rev. A **28**, 2693 (1983).
[21] S. T. Chen and A. C. Gallagher, Phys. Rev. A **17**, 551 (1978).
[22] C. K. Kwan, W. E. Kauppila, R. A. Lukaszew, S. P. Parikh, T. S. Stein, Y. J. Wan, and M. S. Dababneh, Phys. Rev. A **44**, 1620 (1991).
[23] N. Ludwig, A. Bauch, P. Nab, E. Reichert, and W. Welker, Z. Phys. D **4**, 177 (1986).
[24] D. L. Moores and D. W. Norcross, J. Phys. B **5**, 1482 (1972).
[25] I. C. Percival and M. J. Seaton, Philos. Trans. R. Soc. London Ser. A **251**, 113 (1958).
[26] D. R. Flower and M. J. Seaton, Proc. Phys. Soc. London **91**, 59 (1967).
[27] W. Gehenn and M. Wilmers, Z. Phys. **244**, 395 (1971).
[28] W. Williams and S. Trajmar, J. Phys. B **10**, 1955 (1977).
[29] Nils Andersen, Jean W. Gallagher, and Ingolf V. Hertel, Phys. Rep. **165**, 1 (1988).
[30] C. E. Moore, *Atomic Energy Levels*, Natl. Bur. Stand. (U.S.) Circ. No. 467 (U.S. GPO, Washington, DC, 1949), Vol. 1.